Effect of Organoclay Platelets on Morphology of Nylon-6 and Poly(ethylene-*ran*-propylene) Rubber Blends

B. B. Khatua, Dong Jun Lee, Hwang Yong Kim, and Jin Kon Kim*

Department of Chemical Engineering and Polymer Research Institute,
Electronic and Computer Engineering Divisions, Pohang University of Science and Technology,
Pohang, Kyungbuk 790-784, Korea

Received August 14, 2003; Revised Manuscript Received January 17, 2004

ABSTRACT: The effect of organoclay platelets on morphologies of three blend compositions (80/20, 20/80, and 99.5/0.5 w/w) of nylon-6 (N6) and poly(ethylene-*ran*-propylene) rubber (EPR) has been studied by scanning and transmission electron micrographs. For the 80/20 (w/w) N6/ERP blend, the dispersed domain size (*D*) of EPR phase in the N6 matrix decreased significantly even if a small amount of the organoclay was added. The extent of the decrease in *D* in this blend was similar to N6/EPR blend with an in-situ reactive compatibilizer of EPR-*g*-maleic anhydride. The *D* of the blend with the clay did not change upon further annealing at high temperatures, which suggests that the clay seems to be an effective compatibilizer. But, for the 20/80 (w/w) N6/EPR blend, dispersed N6 domain did not decrease with increasing the amount of the clay up to 2 wt %. Moreover, the dispersed N6 domains were not stable against further annealing at high temperatures; thus, coalescence of N6 domains was observed. Furthermore, for 99.5/0.5 (w/w) N6/EPR blend dispersed EPR domains did not change with the amount of the clay. The results indicate that as long as the clay becomes exfoliated in the matrix, the exfoliated clay plates effectively prevent the coalescence of the dispersed domains.

I. Introduction

Blending two or more polymers is a novel technique for producing balanced properties for a specific end use. But, because of thermodynamic immiscibility of polymers, the use of polymer blends has been limited in industry. Thus, either block (or graft) copolymers as physical compatibilizer or in-situ reactive compatibilizers have been employed to improve interfacial adhesion as well as to reduce the dispersed domain in incompatible polymer blends.[1−12]

Recently, clays have been extensively used for preparing nanocomposites having excellent thermal and mechanical properties compared with inorganic filler-based polymer composites.[13−15] Several polymers, for instance, polyamide 6 (N6),[16] polystyrene (PS),[17] poly(methyl methacrylate) (PMMA),[18] poly(propylene) (PP),[19,20] poly(ethylene oxide) (PEO),[21] epoxy,[22] and polymer liquid crystal,[23] have been employed. Lee and Han[24,25] have studied the effect of the compatibility between polymer matrix and organoclay on the rheological properties of polymer/clay nanocomposites. Depending upon the interaction between the clay and the polymer, three different types of nanocomposites are known: phase-separated, intercalated, and exfoliated structures.

Some research groups showed that organoclays could play a role as a compatibilizer for immiscible polymer blends.[26−29] Voulgaris and Petridis[26] showed that the organoclay plays the role of emulsification in the PS/poly(ethyl methacrylate) blend. Gelfer et al.[27] showed that the domain size for PS/PMMA blend was drastically reduced with the addition of organoclay. They explained this behavior by the combination of partial compatibilization by excessive surfactant in organoclays and increased viscosity. On the other hand, Wang et al.[28] reported that the decreased domain size in PS/PP blend by the addition of organoclay was attributed to the fact that two immiscible polymer chains can exist together between the intercalated clay platelets; thus, these two chains play the role of block (or graft) copolymers. However, since the amount of the organoclay added to all of immiscible blends was rather large (up to 30 wt %), the increased viscosity due to the clay should affect the final domain size. Also, all components in the above blends can only intercalate organoclay platelets. Thus, the exact mechanism behind the compatibilization effect has not been elucidated. Recently, Kamal et al.[29] showed that the addition of 5 wt % clay to high-density polyethylene/N6 blend reduced the disperse N6 domains, and the dispersed domain was changed from spherical to laminar shape. On the other hand, Yurekli et al.[30,31] reported that the phase behavior of deuterated PS/poly(vinyl methyl ether) blend exhibiting a lower critical solution transition does not much change even when the amount of an organoclay added was increased to 4 vol %. However, the kinetics and morphological development of phase separation of this blend are significantly influenced by the addition of the organoclay.

In this study, we investigate the role of organoclay platelets on two immiscible polymer blends of nylon-6/poly(ethylene-*ran*-propylene) rubber (EPR). The rationale behind choosing N6/EPR blend is that N6 chains are well-known to exfoliate organic silicate layers,[16] whereas EPR chains intercalate the silicate layers. Once the clay layers are completely exfoliated in the matrix component, the coalescence between dispersed domains is severely reduced due to the presence of exfoliated layers. We found that when a small amount of the clay (less than 0.5 wt %) was added to the blend, the dispersed domain size of EPR phase decreased significantly, and the morphology of the blend prepared by melt blending was very stable against coalescence upon further annealing at high temperatures. Here, we report on our highlights.

---

* To whom correspondence should be addressed: e-mail jkkim@postech.ac.kr; Tel +82-54-279-2276; Fax +82-54-279-8298.

10.1021/ma0352072 CCC: $27.50

II. Experimental Section

Nylon-6 (N6) used in this study was of commercial grade (type L, LG Chemical Co., Korea). Another nylon-6 (N6-H) (KN 120, Kolon Industries, Inc., Korea) with higher viscosity than N6 was also employed. Poly(ethylene-*ran*-propylene) rubber (EPR) was of commercial grade (KEP-020P, KUMHO Polychem Co., Korea) with M_n and M_w of 65 000 and 120 000, respectively. The ethylene content in the EPR was 40 wt %, and the glass transition temperature (T_g) of the EPR was −45 °C. Maleic anhydride grafted EPR (EPR-M) was of commercial grade (MF-416D, Du Pont Co.) having 0.5−1.0 wt % of maleic anhydride.

The organoclay employed in this study was Cloisite 20A (Southern Clay Product Inc). It is a montmorillonite modified with dimethyl dihydrogenated tallow ammonium to increase the domain (d) spacing of Na^+−montmorillonite. The cation exchange capacity (CEC) of Cloisite 20A is 95 mequiv/100 g. Hereafter, Cloisite 20A is referred to as the clay.

Three blend compositions (80/20, 20/80, and 99.5/0.5 (w/w) N6/EPR) with various amounts of the clay (0−10 phr) were prepared by melt-blending at 250 °C and 60 rpm for 20 min with an internal mixer (Brabender Co.) having a capacity of 30 cm^3. Before melt mixing, all polymers and the clay were completely dried in a vacuum oven at 80 °C for 24 h. We also prepared N6/EPR blends with various amounts of EPR-M by melt blending at 250 °C. Previously, we reported that EPR-M was an effective compatibilizer of N6/EPR blends since the reaction between maleic anhydride and amine (or amide) occurs easily.[32]

A field emission scanning electron microscope (S-4200, Hitachi) was used to study the phase morphology of the specimens. The specimens were carefully broken at liquid nitrogen atmosphere. For the 80/20 (w/w) N6/EPR blend, the dispersed phase of EPR was selectively etched out by toluene for 18 h at room temperature, whereas for the 20/80 (w/w) N6/EPR blend, the dispersed phase of N6 was selectively etched out by formic acid for 24 h. Then, the specimens were coated with a thin layer of gold. The number-average (D_n) and the volume-to-surface area average (D_{vs}) domain diameters were obtained with a Quantimet 570 image analyzer (Cambridge instruments). The cross-sectional area (A_i) of each particle in the SEM micrograph was measured and then converted into the diameter (D_i) of a circle having the same cross-sectional area by using the following relation.

$$D_i = 2(A_i/\pi)^{1/2} \qquad (1)$$

Then, D_n and D_{vs} were obtained by

$$D_n = \sum D_i/N$$

$$D_{vs} = \sum D_i^3/\sum D_i^2$$

where N is the total number of dispersed domains (200−300) observed in the SEM images.

The location of the clay in the blend was studied by transmission electron microscopy (TEM: JEOL 1200) operating at an accelerating voltage of 120 kV. Blend samples were ultra-microtomed at cryogenic condition with a thickness of ~50 nm. Owing to different electron contrasts between N6 and EPR, staining was not needed. Since the clay has much higher electron density than neat polymers, it appeared dark in TEM images.

The d spacing of the layer structure of the clay itself as well as that in N6/EPR blends was examined by using a wide-angle X-ray diffractometer (WAXD) with nickel-filtered Cu Kα line (λ = 0.154 04 nm) operated at 40 kV × 100 mA and a scanning rate of 2 deg/min. The sample-to-detector distance was 400 mm.

Using an Advanced Rheometrics Expansion System (ARES) with parallel plates of 25 mm diameter, a frequency sweep experiment for neat N6, EPR, and N6/EPR nanocomposites was done at 250 °C under a nitrogen environment. The strain amplitude (γ_0) was 0.03, which lies in the linear viscoelastic regime.

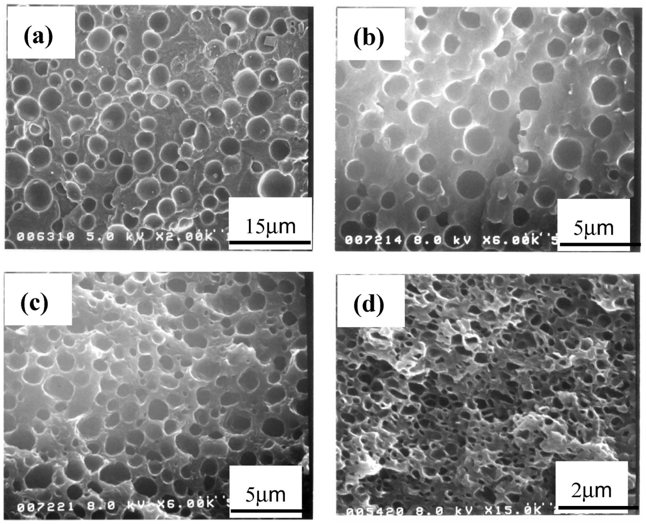

Figure 1. SEM images of 80/20 (w/w) N6/EPR blends with various amounts of the clay. The amount of the clay (in phr) is (a) 0, (b) 0.5, (c) 2, and (d) 10.

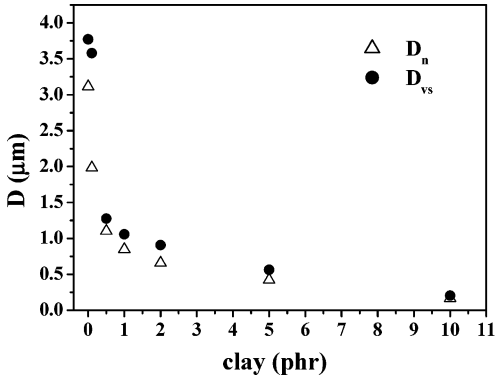

Figure 2. Plot of D_n and D_{vs} of the 80/20 (w/w) N6/EPR blend vs the amount of the clay.

III. Results and Discussion

Figure 1 shows the SEM images of 80/20 (w/w) N6/EPR blends with various amounts of the clay. Interestingly, when a very small amount of clay (0.5 part per hundred (phr)) is used, the dispersed domain size (D) of EPR phase decreases a quarter of that without the clay. As the amount of the clay increases, the D becomes smaller although the decrease rate is much smaller. This indicates that the organoclay plays an important role in reducing the dispersed domain sizes of N6/EPR blends. On the basis of SEM images, the plots of D_n and D_{vs} vs the amount of the clay are shown in Figure 2. It can be seen that a rapid decrease in D was found at lower amounts of the clay, and then a slow but gradual decrease in D was observed with further increasing the amount of the clay. This curve is similar to the emulsification curve, which has been reported for an immiscible blend with a block (or graft) copolymer.[33]

We prepared the 80/20 (w/w) N6/EPR blend with different amounts of EPR-M as a reactive compatibilizer to compare the decrease in D of both systems. The change of D (D_n and D_{vs}) with the amount of EPR-M, shown in Figure 3, is very similar to the 80/20 (w/w) N6/EPR blend with various amounts of the clay. For

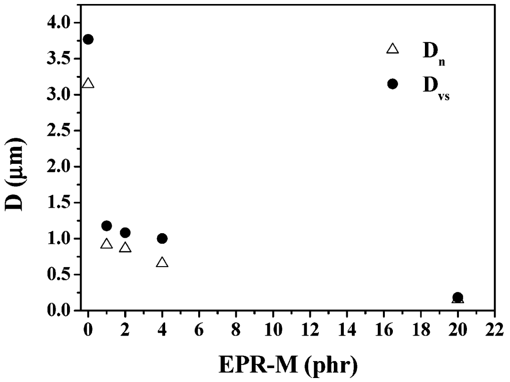

Figure 3. Plot of D_n and D_{vs} of the 80/20 (w/w) N6/EPR blend vs the amount of the ERR-MAH.

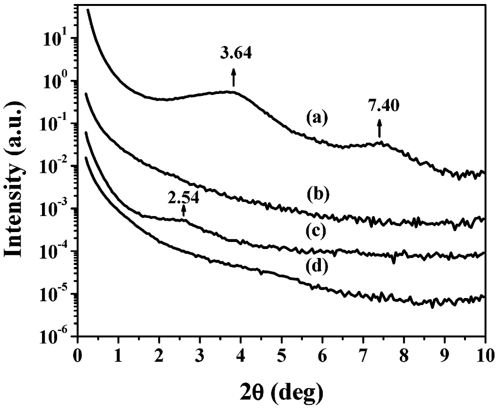

Figure 4. WAXD profiles of the clay itself (a) and various nanocomposites. (b) N6/clay, (c) EPR/clay, (d) 80/20 (w/w) N6/EPR/clay. All nanocomposites contained 5 phr of the clay.

instance, a rapid decrease in *D* was observed at lower amounts of EPR-M. Then, with further increasing the amount of EPR-M, *D* decreased slowly.

To investigate why *D* of the blend decreases with increasing amount of the clay, we first consider the clay dispersion in neat polymers as well as the blend. Figure 4 gives WAXD profiles of the clay itself and the nanocomposites with N6, EPR, and 80/20 (w/w) N6/EPR blend. It is seen in Figure 4 that the clay itself exhibited the characteristic peak at a 2θ of 3.64°, corresponding to *d* spacing of 2.42 nm. For N6/clay nanocomposites, the characteristic peak of the clay did not appear even at smallest value of 2θ of 0.5°, which is the lower limit of the WAXD. This indicates that the clay plates are completely exfoliated by the N6 chains, consistent with previous results.[34−36] On the other hand, for EPR/clay nanocomposites, the characteristic peak of the clay shifted toward lower degree ($2\theta \sim 2.54°$), which suggests that EPR chains only intercalated the clay with the gallery height of 3.48 nm. Finally, the nanocomposite of 80/20 (w/w) N6/EPR blends with 5 phr of the clay did not exhibit any characteristic peak of the clay. Also, when the EPR disperse phases in the 80/20 (w/w) N6/EPR blend were completely etched out by toluene, WAXD profiles of the clay remained the same.

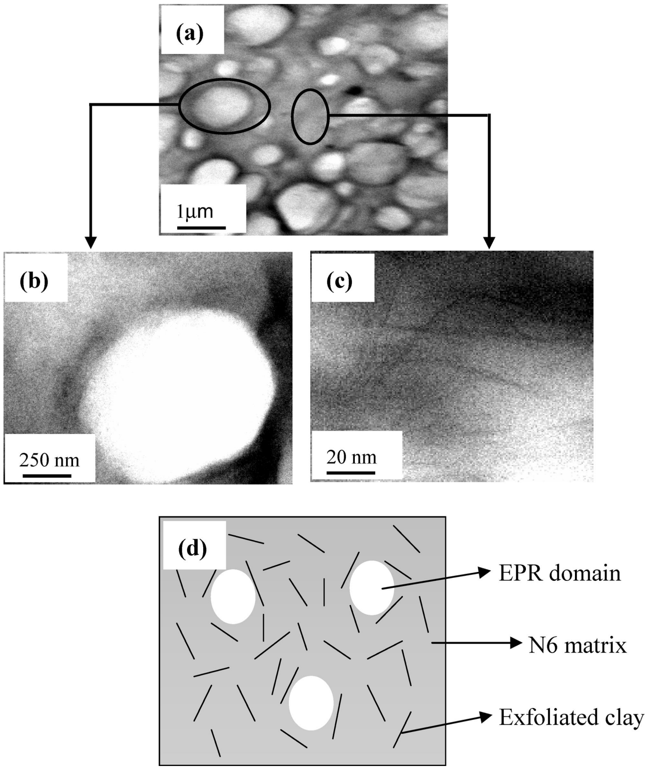

Figure 5. TEM images of 80/20 (w/w) N6/EPR blends with 1 phr of the clay: (a) lower magnification, (b) higher magnification of EPR domain, (c) higher magnification of N6 matrix, (d) schematic for the role of the clay platelets on the immiscible polymer blend. The white area represents the EPR phase.

Figure 5 shows TEM images of the 80/20 (w/w) N6/EPR blend with 1 phr of the clay. The white dispersed domains correspond to the EPR phases, and the domain size is in agreement with that obtained from SEM (see Figure 2). Since we could not see any discernible clay platelets in EPR domains as well as N6/EPR interface, as shown in Figure 5b, we consider that almost all clay platelets exist in the N6 matrix with full exfoliation (Figure 5c), although it is not completely excluded that a very small amount of the intercalated clay might exist in the EPR dispersed phase. The preference of the clay existing in the N6 matrix is due to the difference in miscibility between organoclay with polymer chains.[37,38] N6 chain is more polar than EPR chain; thus, the silicate layers are easily exfoliated by N6 chains compared with EPR chains. On the basis of these results, we drew a schematic of the role of exfoliated clay on N6/EPR blend in Figure 5d. Since the exfoliated clay platelets are mostly located in the nylon-6 matrix, these could act as barriers to prevent the coalescence of the EPR domains.

Furthermore, the morphology of 80/20 (w/w) N6/EPR blends with the clay was very stable upon annealing at high temperatures. Figure 6 gives SEM images of 80/20 (w/w) N6/EPR blends without and with 2 phr of the clay after a long annealing (4 h) at 250 °C. Compared with Figure 1, D_{vs} of the blend without the clay increased with annealing (from 3.8 to 4.9 μm), as consistent with incompatible polymer blends.[39,40] However, when the organoclay was present, the D_{vs} (or D_n) did not change with annealing time. Once the above scenario for the role of the clay is right, we expect that the clay cannot act as an effective barrier for another blend composition where exfoliated platelets are present in the dispersed domains.

For this purpose, we prepared 20/80 (w/w) N6/EPR blend in which the N6 phase becomes dispersed domains. Figure 7 gives SEM images for 20/80 (w/w) N6/EPR blends without and with 2 phr of the clay. As shown in Figure 7b, even if 2 phr of the clay is added to 20/80 (w/w) N6/EPR blend, the D_{vs} of the dispersed phase (N6) is 3.7 μm, which is almost same as that (3.6 μm) without the clay. This is quite a contrast to the 80/

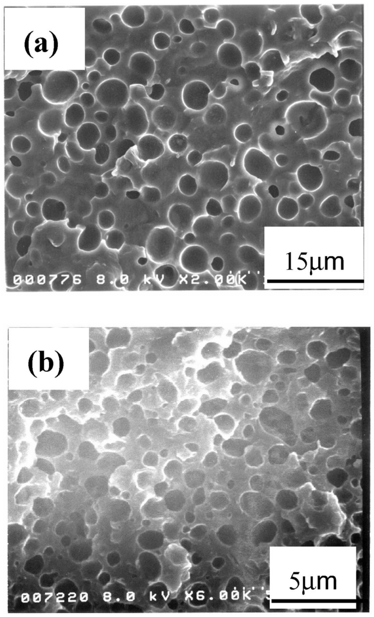

Figure 6. SEM images of 80/20 (w/w) N6/EPR blends after annealing at 250 °C for 4 h: (a) without the clay, (b) with 2 phr of the clay.

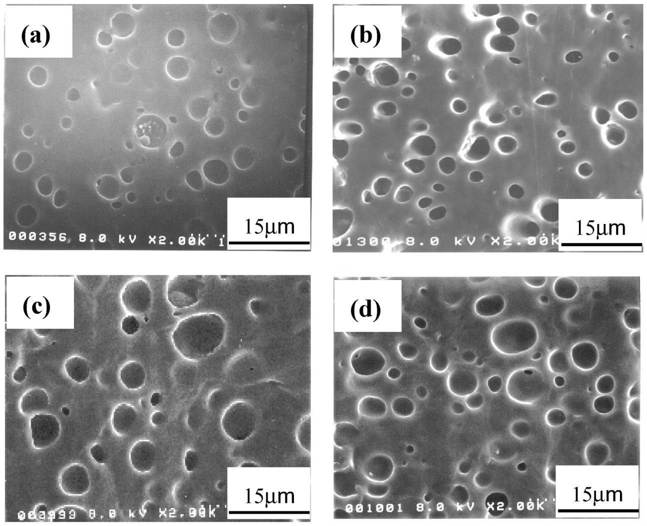

Figure 7. SEM images of 20/80 (w/w) N6/EPR blends before (a, b) and after annealing (c, d) at 250 °C for 4 h: (a, c) without clay, (b, d) with 2 phr of the clay.

20 (w/w) N6/EPR blend, where the D_{vs} of EPR domain in the 80/20 (w/w) N6/EPR blend with 2 phr of the clay was 0.9 μm, which is significantly smaller than that (3.8 μm) without the clay. Furthermore, when 20/80 (w/w) N6/EPR blend with 2 phr of the clay was annealed at 250 °C for 4 h, D_{vs} increased significantly (5.6 μm) (Figure 7d), which is the same as that without the clay.

But, with further increasing amount of clay, dispersed N6 domains began to decrease. For instance, D_{vs} of the 20/80 (w/w) N6/EPR blend with 5 phr of clay was 1.1 μm. The decrease in D with increasing clay loading is due to the increased viscosity of the EPR matrix. However, D_{vs} of this blend increased to 3.2 μm when annealed at 250 °C for 4 h. Thus, these results clearly demonstrate that the morphology of the 20/80 (w/w) N6/EPR blend with the clay was not stable against annealing. This is because almost all clays were located inside the dispersed N6 phase, which was evident by the fact that any WAXD peak corresponding to the clay in the 20/80 (w/w) N6/EPR blend was not observed. Furthermore, the TEM image of the 20/80 (w/w) N6/EPR blend with 1 phr of the clay, as given in Figure 8, clearly showed that exfoliated platelets existed only inside N6 domains. In this situation, dispersed N6 domains could easily be coalesced since there were not exfoliated platelets in the EPR matrix. Thus, we consider that the exfoliated platelets locating inside the dispersed domains do not act effectively as a barrier for the coalescence of the dispersed domains.

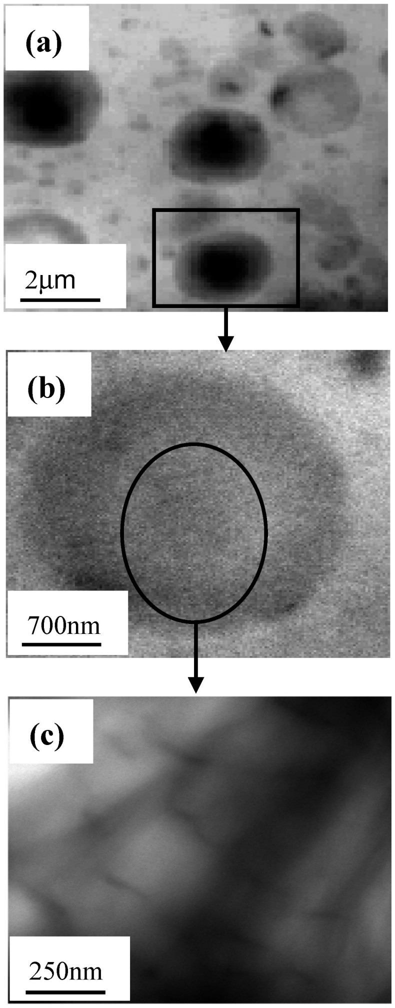

Figure 8. TEM images 20/80 (w/w) N6/EPR blends with 1 phr of the clay: (a) lower magnification, (b, c) higher magnification of N6 domain.

Recently, Wang et al.[28] reported the compatibility effect of an organoclay in the 70/30 (w/w) PP/PS blend. However, they did not show the stability of morphology of this blend upon annealing at high temperatures. To investigate the stability of the morphology of PP/PS blend with the clay, we performed annealing experiment on 70/30 (w/w) PP/PS blends with different amounts (2−5 phr) of clay. The weight-average molecular weights and polydispersity indices are 160 000 and 3.5 for PP (PP 5030; Korea Petrochem. Ind. Co.) and 230 000 and 1.64 for PS (Aldrich Chem.), respectively. We found that D_n of dispersed PS domains of the blend with 5 phr of the clay was 3.96 μm, which is smaller than that (6.41 μm) of the blend without the clay. This is qualitatively agreement with results in ref 28. However, D_n of 70/30 (w/w) PP/PS blend with 5 phr was increased to 6.9 μm upon annealing at 210 °C for 6 h, indicating clearly that the coalescence of PS domains occurred. Thus, we

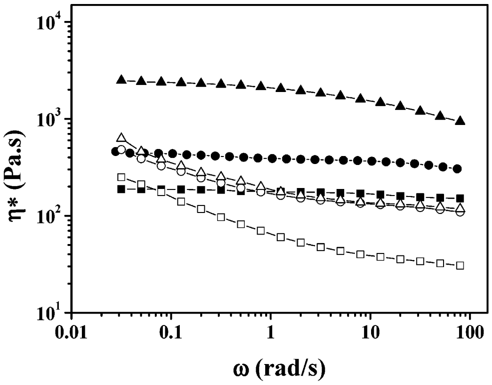

Figure 9. Plot of complex viscosity (η*) with frequency (ω) at 250 °C: (■) N6; (●) N6-H; (▲) EPR; (□) 80/20 (w/w) N6/EPR blend; (△) 80/20 (w/w) N6/EPR blend with 1 phr of the clay; (○) 80/20 (w/w) N6-H/EPR blend without the clay.

consider that the reduction in the PS domains in PP/PS blend by the addition of the clay resulted mainly from the increased matrix viscosity, not from the compatibilization effect of the clay locating at the interface.

One can argue that the decreased domain size in the 80/20 (w/w) blend by the addition of the clay might be attributed to the increased viscosity by the clay. When the viscous force becomes stronger, it is known that the *D* of a blend prepared by melt mixing becomes smaller.[41] To check this possibility, we measured the complex viscosities (η*) of neat N6, EPR, and 80/20 (w/w) N6/EPR blend without and with the clay, as shown in Figure 9. It was seen that η* of the 80/20 (w/w) N6/EPR blend increased by the addition of 1 phr of the clay. Thus, the decrease in *D* of dispersed EPR domains in the 80/20 (w/w) N6/EPR/clay nanocomposite may be due to increased viscosity of matrix phase (N6). To clarify the effect of matrix viscosity on morphology of the 80/20 (w/w) N6/EPR blend, we also investigated the blend morphology with another N6 (N6-H) with 30% higher viscosity than that of N6, as shown in Figure 9. Thus, the viscosity of the 80/20 (w/w) N6-H/EPR blend exhibited almost the same as that of the 80/20 (w/w) N6/EPR blend with 1 phr of the clay at the entire frequencies (0.1−100 rad/s). We observed that the D_n of the 80/20 (w/w) N6-H/EPR blend was 1.7 μm, which is smaller than that (3.1 μm) of the 80/20 (w/w) N6/EPR blend. But, as shown previously, the D_n of the 80/20 (w/w) N6/EPR blend with 1 phr clay was 0.84 μm. Moreover, when the 80/20 (w/w) N6-H/EPR blend was annealed at 250 °C for 4 h, D_n increased significantly (3.2 μm); thus, the morphologies are not stable against annealing. These results lead us to conclude that the main effect of the decrease in *D* in the 80/20 (w/w) N6/EPR blend in the presence of the clay is not due to the increased viscosity of the matrix polymer but due to the barrier effect for preventing coalescence of the dispersed phase.

To study the barrier effect of organoclay on the immiscible blend, we also studied the morphology of 99.5/0.5 (w/w) N6/EPR blends without and with the clay. We found that this blend composition did not exhibit any coalescence of the dispersed EPR domains. Figure 10 shows SEM imaged of these blends. It is seen in Figure 10 that D_n for 99.5/0.5 (w/w) N6/EPR blend without the clay was 0.61 μm, which is significantly smaller than that (3.11 μm) for the 80/20 (w/w) N6/EPR blend. However, D_n of the 99.5/0.5 (w/w) N6/EPR blend with 1 phr of the clay was 0.58 μm, which is almost the same that without the clay. When the amount of the clay increased to 5 phr, D_n was 0.45 μm. This clearly indicates that the clay did not play a role of the compatibilizer similar to block (or graft) copolymers in immiscible polymer blends. A slight decrease in D_n for the 99.5/0.5 (w/w) N6/EPR blend with 5 phr of the clay is due to the increased viscosity of the matrix phase.

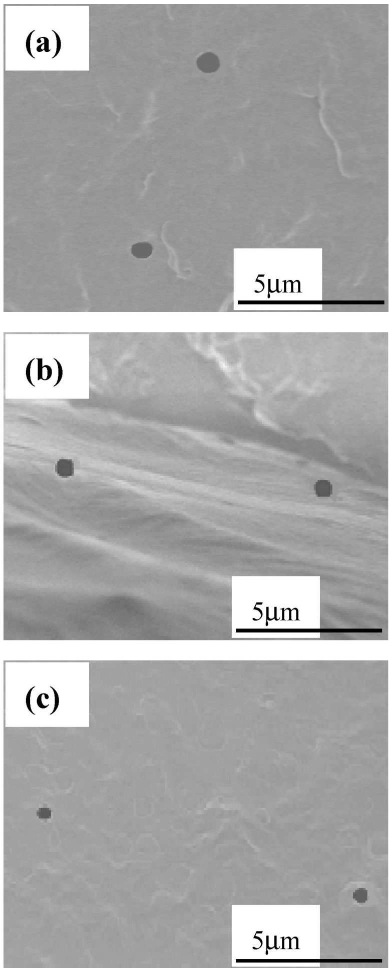

Figure 10. SEM images of 99.5/0.5 (w/w) N6/EPR blends with various amounts of the clay. The amount of the clay (in phr) is (a) 0, (b) 1, and (c) 5.

Finally, we investigated the impact strength of 80/20 (w/w) N6/EPR blends without and with EPR-M and the clay. We found that the D_n of 80/20 (w/w) N6/EPR with 2 phr of the clay was 0.66 μm, which is close to that (0.65 μm) of the 80/16/4 (w/w/w) N6/EPR/EPR-M blend without the clay. But, the impact strength of the former blend was 76 J/m, which was much smaller than that (140 J/m) of the latter. The increased impact strength for the latter blend is the increased interfacial adhesion resulting from the generation of EPR-*g*-N6 copolymers in the interface. When there was no EPR-M, the impact strength of the 80/20 (w/w) N6/EPR blend did not change even when 5 phr of the clay was added to the blend. This clearly indicates that the clay does not improve the interfacial adhesion between N6 and ERP phases, whereas EPR-M does. Thus, the exfoliated organoclay platelets play a main role in preventing the coalescence of the dispersed domains, thus reducing dispersed domain sizes. However, the decrease in the dispersed domain size by the addition of the organoclay does not mean the increased compatibility between two immiscible polymer chains.

IV. Conclusion

In this study, we have shown that an organoclay plays an important role in reducing the dispersed domain sizes in incompatible polymer blends of N6/EPR blends. The average diameter size of the dispersed EPR domains in 80/20 (w/w) N6/EPR blends decreases significantly even when a small amount (0.5 phr) of the clay is added. According to TEM images, we concluded that almost all of exfoliated clay platelets existed in the N6 matrix. Interestingly, when EPR becomes the matrix phase for the 20/80 (w/w) N6/EPR blend, dispersed N6 domain does not decrease with increasing the amount of clay up to 2 wt %. We concluded that exfoliated clay platelets in the polymer matrix effectively prevented the coalescence of dispersed domains, resulting in the decreased domains. However, the decrease in the dispersed domain size by the addition of the organoclay does not suggest the increase in the compatibility (or miscibility) between two immiscible polymer chains since the organoclay platelets are not located near the interface.

Acknowledgment. Cloisite 20A was kindly supplied by Southern Clay Co. This work was supported by the Korea Research Foundation (KRF-20020005-D0008).

References and Notes

(1) Bucknall, C. B. *Toughened Plastics*; Applied Science Publishers: London, 1977.
(2) Folkes, M. J.; Hope, P. S. *Polymer Blends and Alloys*, 1st ed.; Blackie Academic and Professional An imprint of Chapman & Hall: London, UK, 1993.
(3) Utracki, L. A. In *Polymer Alloys and Blends*; Hanser Publishers: Munich, 1989.
(4) Olabisi, O.; Robeson, L. M.; Shaw, M. T. In *Polymer−Polymer Miscibility*; Academic Press: New York, 1979.
(5) Paul, D. R.; Newman, S. In *Polymer Blends*; Academic Press: New York, 1978; Vol. 2.
(6) Lohse, D. J. In *Polymeric Materials Encyclopedia*; Salamone, J. C., Ed.; CRC Press: New York, 1996; Vol. 2.
(7) Utracki, L. A. In *Commercial Polymer Blends*; Chapman & Hall Press: London, 1998.
(8) Deanin, R. D.; Manion, M. A. In *Polymer Blends and Alloys*; Marcel Dekker: New York, 1999.
(9) Brown, H. R. *Macromolecules* **1989**, *22*, 2859.
(10) Fayt, R.; Jerome, R.; Teyssie, Ph. *J. Polym. Sci., Polym. Phys.* **1989**, *27*, 775.
(11) Kim, J. K.; Kim. S.; Park, C. E. *Polymer* **1997**, *38*, 2155.
(12) Xanthos, M.; Dagli, S. S. *Polym. Eng. Sci.* **1991**, *31*, 929.
(13) Giannelis, E. P. *Adv. Mater.* **1996**, *8*, 29.
(14) LeBaron, P. C.; Wang, Z.; Pinnavaia, T. *J. Appl. Clay Sci.* **1999**, *15*, 11.
(15) Vaia, R. A.; Jandt, K. D.; Kramer, E. J.; Giannelis, E. P. *Macromolecules* **1995**, *28*, 8080.
(16) Fornes, T. D.; Yoon, P. J.; Hunter, D. L.; Keskkula, H.; Paul, D. R. *Polymer* **2002**, *43*, 5915.
(17) Fu, X.; Qutubuddin, S. *Polymer* **2001**, *42*, 807.
(18) Huang, X. Y.; Brittain, W. J. *Macromolecules* **2001**, *34*, 3255.
(19) Hambir, S.; Bulakh, N.; Jog, J. P. *Polym. Eng. Sci.* **2002**, *42*, 1800.
(20) Zhang, Q.; Wang, Y.; Fu, Q. *J. Polym. Sci., Polym. Phys.* **2003**, *41*, 1.
(21) Bujdak, J.; Hackett, E.; Giannelis, E. P. *Chem. Mater.* **2000**, *12*, 2168.
(22) Park, J. H.; Jana, S. C. *Macromolecules* **2003**, *36*, 2758.
(23) Vaia, R. A.; Giannelis, E. P. *Polymer* **2001**, *42*, 1281.
(24) Lee, K. M.; Han, C. D. *Macromolecules* **2003**, *36*, 7165.
(25) Lee, K. M.; Han, C. D. *Polymer* **2003**, *44*, 4573.
(26) Voulgaris, D.; Petridis, D. *Polymer* **2002**, *43*, 2213.
(27) Gelfer, M. Y.; Song, H. H.; Liu, L.; Hsiao, B. S.; Chu, B.; Rafailovich, M.; Si, M.; Zaitsev, V. *J. Polym. Sci., Polym. Phys.* **2003**, *41*, 44.
(28) Wang, Y.; Zhang, Q.; Fu, Q. *Macromol. Rapid Commun.* **2003**, *24*, 231.
(29) Mehrabzadeh, M.; Kamal, M. R. *Can. J. Chem. Eng.* **2002**, *80*, 1083.
(30) Yurekli, K.; Karim, A.; Amis, E. J.; Krishnamoorti, R. *Macromolecules* **2003**, *36*, 7256.
(31) Yurekli, K.; Karim, A.; Amis, E. J.; Krishnamoorti, R. *Macromolecules*, **2004**, *37*, 507.
(32) Kim, J. K.; Park, S. H.; O, H. T.; Jeon, H. K. *Polymer* **2001**, *42*, 2209.
(33) Favis, B. D. *Polymer* **1994**, *35*, 1532.
(34) Usuki, A.; Kojima, Y.; Kawasumi, M.; Okada, A.; Fukushima, Y.; Kurauchi, T.; Kamigaito, O. *J. Mater. Res.* **1993**, *8*, 1179.
(35) Liu, L.; Qi, Z.; Zhu, X. *J. Appl. Polym. Sci.* **1999**, *71*, 1133.
(36) Fornes, T. D.; Yoon, P. J.; Keskkula, H.; Paul, D. R. *Polymer* **2002**, *43*, 2121.
(37) Alexandre, M.; Dubois, P. *Mater. Sci. Eng. R* **2000**, *28*, 1.
(38) Giannelis, E. P.; Krishnamoorti, R.; Manias, E. *Adv. Polym. Sci.* **1999**, *138*, 107.
(39) Sundararaj, U.; Macosko, C. W. *Macromolecules* **1995**, *28*, 2647.
(40) Macosko, C. W.; Guegan, P.; Khandpur, A. K. *Macromolecules* **1996**, *29*, 5590.
(41) Han, C. D. *Multiphase Flow in Polymer Processing*; Academic Press: New York, 1981; Chapter 4.

MA0352072